

ANNALES DE LA FACULTÉ DES SCIENCES DE TOULOUSE Mathématiques

CHRISTIANE ROUSSEAU

Two-parameter unfolding of a parabolic point of a vector field in \mathbb{C} fixing the origin

Tome XXX, n° 1 (2021), p. 139–169.

<https://doi.org/10.5802/afst.1669>

© Université Paul Sabatier, Toulouse, 2021.

L'accès aux articles de la revue « Annales de la faculté des sciences de Toulouse Mathématiques » (<http://afst.centre-mersenne.org/>) implique l'accord avec les conditions générales d'utilisation (<http://afst.centre-mersenne.org/legal/>). Les articles sont publiés sous la licence CC-BY 4.0.



Publication membre du centre
Mersenne pour l'édition scientifique ouverte
<http://www.centre-mersenne.org/>

Two-parameter unfolding of a parabolic point of a vector field in \mathbb{C} fixing the origin ^(*)

CHRISTIANE ROUSSEAU ⁽¹⁾

ABSTRACT. — In this paper we describe the bifurcation diagram of the 2-parameter family of vector fields $\dot{z} = z(z^k + \epsilon_1 z + \epsilon_0)$ over \mathbb{CP}^1 for $(\epsilon_1, \epsilon_0) \in \mathbb{C}^2$. There are two kinds of bifurcations: bifurcations of parabolic points and bifurcations of homoclinic loops through infinity. The latter are studied using the tool of the periodgon introduced in a particular case in [1], and then generalized in [4]. We apply the results to the bifurcation diagram of a generic germ of 2-parameter analytic unfolding preserving the origin of the vector field $\dot{z} = z^{k+1} + o(z^{k+1})$ with a parabolic point at the origin.

RÉSUMÉ. — Dans cet article nous décrivons le diagramme de bifurcation de la famille de champs de vecteurs à deux paramètres $\dot{z} = z(z^k + \epsilon_1 z + \epsilon_0)$ sur \mathbb{CP}^1 pour $(\epsilon_1, \epsilon_0) \in \mathbb{C}^2$. Il y a deux types de bifurcations: des bifurcations de points paraboliques et des bifurcations de boucles homocliniques par le pôle à l’infini. Ces dernières sont étudiées en utilisant l’outil du polygone des périodes introduit dans un cas particulier dans [1] et généralisé dans [4]. On applique les résultats au diagramme de bifurcation d’un germe générique de déploiement analytique à deux paramètres préservant l’origine du champ de vecteurs $\dot{z} = z^{k+1} + o(z^{k+1})$ avec un point parabolique à l’origine.

1. Introduction

This paper is part of a larger program to explore the dynamics of polynomial vector fields on \mathbb{C} depending on a small number m of parameters, which appear as “generic models” of the unfolding of a parabolic point $\dot{z} = \frac{dz}{dt} = z^{k+1} + o(z^{k+1})$ of codimension k (i.e. multiplicity $k + 1$). The

^(*) Reçu le 11 décembre 2018, accepté le 13 juin 2019.

2020 *Mathematics Subject Classification*: 37F75, 32M25, 32S65, 34M99.

⁽¹⁾ Département de mathématiques et de statistique, Université de Montréal, C.P. 6128, Succursale Centre-ville, Montréal (Qc), H3C 3J7, Canada — christiane.rousseau@umontreal.ca

The author is supported by NSERC in Canada.

Article proposé par Marie-Claude Arnaud.

paper [1] studied the case $m = 1$, and the paper [4], the case $m = 2$. When $m = 1$, the singular points of $\dot{z} = z^{k+1} + \epsilon$ are located at the vertices of a regular polygon. For $m = 2$, the family of vector fields $\dot{z} = z^{k+1} + \epsilon_1 z + \epsilon_0$ shows the transition between the case $\epsilon_1 = 0$ described in [1] and the case $\epsilon_0 = 0$ which has one singular point at the origin surrounded by k singular points located at the vertices of a regular polygon. When one moves from $\epsilon_0 = 0$ to $\epsilon_1 = 0$, the inner point moves outwards in one direction, and the k outer singular points rotate monotonically in inverse directions on both sides of the direction followed by the inner point, so as to leave space for the inner point. This is in line with Khovanskii's fewnomial theory [3], which asserts that polynomials with very few monomials (called *fewnomials*) have roots with very equidistributed arguments (and hence fewnomials with real coefficients have few real roots, regardless of their degree).

One motivation for studying these families of polynomial vector fields is that their time-one maps are good models (at least topologically) for the unfoldings of germs of diffeomorphisms with a parabolic fixed point of codimension k :

$$f(z) = z + z^{k+1} + o(z^{k+1}). \quad (1.1)$$

A good topological model for a generic 1-parameter unfolding is the time-one map of $\dot{z} = z^{k+1} + \epsilon_0$. While the full dynamics that can occur in perturbations of such a diffeomorphism can only be described in generic unfoldings depending on k parameters (see [5]), it is not uncommon that a germ of codimension k is only embedded in a generic family with $m < k$ parameters; and it is natural to study what particular dynamics occurs in such a generic family.

A similar problem is that of studying the unfoldings of germs of diffeomorphisms with a parabolic fixed point of codimension k :

$$g(z) = \exp(2\pi i p/q)z + \frac{1}{q}z^{kq+1} + o(z^{kq+1}). \quad (1.2)$$

The study is often done by considering $f = g^{\circ q}(z)$, which has the form of (1.1) for some new $K = kq$. A significant difference though is the structurally stable fixed point, which can be kept at the origin by an analytic change of coordinate. In the case of (1.2), a generic 1-parameter unfolding of g yields a 1-parameter unfolding of f , which is topologically the time-one map of $\dot{z} = z^{K+1} + \epsilon_1 z$. Hence, it is natural to integrate the two cases in a 2-parameter family and study the family of vector fields $\dot{z} = z^{K+1} + \epsilon_1 z + \epsilon_0$. This is what has been done in [4]. A different problem is to study what occurs in generic 2-parameter unfoldings g_ϵ of g defined in (1.2), through the 2-parameter family $f_\epsilon = g_\epsilon^{\circ q}$. A formal normal form of f_ϵ is given by the

time-one map of a family of polynomial vector fields

$$\begin{aligned} \dot{Z} = v_\eta(Z) &= Z \left(Z^{qk} + \sum_{j=2}^{k-1} b_j(\eta) Z^{jq} + \eta_1 Z^q + \eta_0 \right) R_\eta(Z^q) \\ &= w_\eta(Z) R_\eta(Z^q), \end{aligned} \quad (1.3)$$

where $\eta = (\eta_1, \eta_0) \in (\mathbb{C}^2, 0)$, $\epsilon \mapsto \eta$ is an invertible change of parameter, $b_j(0) = 0$, R_η is a polynomial of degree at most k which is equal to 1 when Z and η vanish, and the b_j depend analytically on η . The case $k = 1$ is done in [7] and the case $k > 1$ in the Appendix. What is typical in classifying families of germs of diffeomorphisms with such a normal form is to make a change of variable to the time-variable

$$t = \int \frac{dz}{w_\eta(Z)},$$

transforming the diffeomorphism to a small perturbation of the translation by 1. This is done on sectors in parameter space determined by the bifurcation diagram of the vector field $\dot{Z} = w_\eta(Z)$.

For each small η , the dynamics and bifurcations of the vector field $\dot{Z} = w_\eta(Z)$ are very close to those of

$$\dot{Z} = Q_\epsilon(Z) = Z(Z^{qk} + \eta_1 Z^q + \eta_0), \quad \eta = (\eta_1, \eta_0) \in (\mathbb{C}^2, 0). \quad (1.4)$$

Hence, as a first step, the paper focuses on describing the bifurcation diagram of the real dynamics of the family (1.4). This family is invariant under rotations of order q .

The change $(z, \epsilon_1, \epsilon_0) = (q^{\frac{1}{k}} Z^q, q^{\frac{k-1}{k}} \eta_1, q \eta_0)$ reduces the family (1.4) to the form

$$\dot{z} = P_\epsilon(z) = z(z^k + \epsilon_1 z + \epsilon_0), \quad \epsilon = (\epsilon_1, \epsilon_0) \in \mathbb{C}^2, \quad (1.5)$$

and it suffices to study the bifurcation diagram of (1.5).

Douady, Estrada and Sentenac pioneered the study of polynomial vector fields on \mathbb{C} : they introduced in [2] a two part invariant composed

- on the one hand, of a combinatorial invariant in the form of a tree graph with $k + 1$ vertices at the singular points,
- and, on the other hand, of an analytic invariant given by a vector in \mathbb{H}^k .

This invariant characterizes *Douady–Estrada–Sentenac generic* (or DES-generic) polynomial vector fields in \mathbb{C} , i.e. polynomial vector fields with simple points and no homoclinic loop through the pole at ∞ : the polynomial vector field with a given Douady–Estrada–Sentenac invariant is unique when

monic and centered (the sum of the roots is zero). In the study of the vector field $\dot{z} = z^{k+1} + \epsilon$, the paper [1] introduced, for each $\epsilon \neq 0$, a new invariant, the *periodgon*, or *polygon of the periods*. The periodgon is a polygon with $k+1$ sides, one for each fixed point, which completely characterizes the polynomial vector field up to a rotation of order k , provided it is monic and centered. The periodgon was later generalized in [4] to all *generic* polynomial vector fields $\dot{z} = dz/dt = P(z)$, where *generic* is understood in a different sense defined below. The periodgon is a polygon whose edges are given by oriented vectors corresponding to the periods of the different singular points of the vector field, in a proper order. It is the boundary of a simply connected closed region in the Riemann surface of the time variable (which is a translation surface). It is uniquely defined on open sets of generic values in the parameter space for which:

- all singular points are simple;
- given any singular point z^* and δ such that $e^{i\delta}P'(z^*) \in i\mathbb{R}^+$, i.e. z^* is a center for the rotated vector field $\dot{z} = e^{i\delta}P(z)$, then the domain of the center, called the *periodic domain* of z^* , is bounded by a unique homoclinic loop through infinity.

These open sets are separated by surfaces in parameter space where the periodic domain of at least one singular point is bounded by several homoclinic loops through infinity. Geometrically, the periodgon is the image in t -space of the complement in \mathbb{CP}^1 of the union of the periodic domains of all singular points.

The bifurcations of a polynomial vector field on \mathbb{C} can be of two types:

- Bifurcations of multiple singular points: these occur on the discriminant locus, an algebraic variety of real codimension 2;
- Bifurcations of homoclinic loops through ∞ : these occur precisely when two vertices of the periodgon are linked by a horizontal segment lying inside it.

Hence the periodgon is a powerful tool to describe the bifurcation diagram. But it is not very easy to compute the periodgon: the difficulty is to determine the order of the edges. This order is the cyclic order around ∞ of the periodic domains at the singular points. The order changes when a periodic domain is bounded by more than one homoclinic loop through ∞ : at these situations, the periodgon still exists, but it is not uniquely defined since several orders are possible. Hence the present paper is also motivated by the need to better understand the periodgon through the study of the system (1.5).

Among the questions we want to consider are the following:

Question 1. — How many open sets in parameter space are needed to describe all generic vector fields? This seems to be less than the number of open sets for the Douady–Estrada–Sentenac description. For instance, for the family $\dot{z} = z^{k+1} + \epsilon$, $2(k+1)$ open sets are needed for the Douady–Estrada–Sentenac description, while one open set is enough with the periodgon description (see [1]). One open set with slits is conjectured to be sufficient with the periodgon description for the family $\dot{z} = z^{k+1} + \epsilon_1 z + \epsilon_0$ (see [4]), while two are necessary for $\dot{z} = z^3 + \epsilon_1 z + \epsilon_0$ with the Douady–Estrada–Sentenac point of view (see [6]). For the family (1.5) we conjecture that $k-1$ open sets are sufficient: these domains are exactly the ones to which we can reduce our study using the symmetries of the system. When k is even, each open set has an additional slit.

Question 2. — Is the periodgon planar or does its projection on \mathbb{C} have self-intersection? The periodgon of $\dot{z} = z^{k+1} + \epsilon$ is planar, while that of $\dot{z} = z^{k+1} + \epsilon_1 z + \epsilon_0$ was conjectured to be planar. Here again we conjecture that the periodgon is planar.

As a natural application we then discuss the bifurcation diagram of a generic germ of 2-parameter analytic unfolding preserving the origin of a vector field $\dot{z} = z^{k+1} + o(z^{k+1})$ with a parabolic point at the origin, whose bifurcation diagram can be described by generalizing the notion of periodgon when the vector field is restricted to a disk.

The paper is organized as follows. In Section 2, we start studying the bifurcation diagram of (1.5) via classical tools. In Section 3, we study the periodgon of (1.5). In Section 4, we give the bifurcation diagram of (1.5). In Section 5 we discuss the bifurcation diagram of a generic germ of 2-parameter analytic unfolding preserving the origin of the vector field $\dot{z} = z^{k+1} + o(z^{k+1})$ with a parabolic point at the origin. The Appendix (Section 6) derives the formal normal form for germs of unfoldings of diffeomorphisms with a parabolic fixed point of codimension k as in (1.2).

2. Study of the phase portrait of (1.5)

2.1. Generalities on polynomial vector fields on \mathbb{C}

Let $\dot{z} = P(z)$ be a polynomial vector field of degree $k+1 \geq 2$ on \mathbb{C} . Then the point at infinity is a pole of order $k-1$ with k attracting and k repelling separatrices. Any finite simple singular point z_j is either a radial node, or a focus, or a center. In particular, it is a center if $P'(z_j) \in i\mathbb{R}$. Since the periodic domain of a center is always bounded by homoclinic loop(s) through infinity, the only bifurcations that can occur are:

- (1) Bifurcations of parabolic point (multiple point) when $P'(z_j) = 0$. Then $P(z_j) = c(z - z_j)^{\ell+1} + o((z - z_j)^{\ell+1})$, and ℓ is called the codimension of the parabolic point;
- (2) Bifurcations of homoclinic loop through ∞ , when an attracting separatrix and a repelling separatrix coalesce;
- (3) And combinations of the previous types.

2.2. Symmetries of the family

We consider the action of the transformation:

$$(z, t, \epsilon_1, \epsilon_0) \mapsto (Z, T, \eta_1, \eta_0) = (Az, A^{-k}t, A^{k-1}\epsilon_1, A^k\epsilon_0) \quad (2.1)$$

on the vector field $\frac{dz}{dt} = P_\epsilon(z)$ in (1.5) with $t \in \mathbb{R}$, changing it to $\frac{dZ}{dT} = P_\eta(Z)$. We will use the particular cases:

- $A = r \in \mathbb{R}^+$. This rescaling allows to suppose that $(\eta_1, \eta_0) \in \mathbb{S}^3 = \{\|\eta\| = 1\}$, for the “norm” introduced below in (2.4).
- $A = e^{\frac{2\pi im}{k}}$. This gives invariance of the vector field under rotations of order k , modulo reparametrization.
- $A = e^{\frac{\pi i(2m+1)}{k}}$. This gives invariance under rotations of exact order $2k$, modulo reparametrization and reversing of time.

PROPOSITION 2.1. — *Let σ be the reflection with respect to the line $e^{\frac{m}{k}\pi i}\mathbb{R}$.*

- (1) *Let P_ϵ and $P_{\epsilon'}$ be of the form (1.5) for $\epsilon = (\epsilon_1, \epsilon_0)$ and $\epsilon' = (\epsilon'_1, \epsilon'_0)$. If*

$$\begin{cases} \epsilon'_1 = e^{-\frac{2m}{k}\pi i}\bar{\epsilon}_1, & m \in \mathbb{Z}_{2k}, \\ \epsilon'_0 = \bar{\epsilon}_0, \end{cases} \quad (2.2)$$

then the vector fields P_ϵ and $P_{\epsilon'}$ are conjugate under the change $z \mapsto \sigma(z)$.

- (2) *In particular, when $\epsilon_0 \in \mathbb{R}$ and $\arg(\epsilon_1) = -\frac{\pi m}{k}$, $m \in \mathbb{Z}_{2k}$, then the system is symmetric with respect to the line $e^{\frac{im\pi}{k}}\mathbb{R}$, i.e. invariant under $z \mapsto \sigma(z)$.*

Proof. — For real t , the reflection $\sigma : z \mapsto Z = e^{\frac{2m}{k}\pi i}\bar{z}$ sends the vector field (1.5) to

$$\frac{dZ}{dT} = Z(Z^k + \bar{\epsilon}_1 e^{-\frac{2m}{k}\pi i} Z + \bar{\epsilon}_0). \quad \square$$

PROPOSITION 2.2. — *Let σ be the reflection with respect to the line $e^{\frac{2m+1}{2k}\pi i}\mathbb{R}$.*

(1) Let P_ϵ and $P_{\epsilon'}$ be of the form (1.5) for $\epsilon = (\epsilon_1, \epsilon_0)$ and $\epsilon' = (\epsilon'_1, \epsilon'_0)$. If

$$\begin{cases} \epsilon'_1 = -e^{-\frac{(2m+1)}{k}\pi i}\bar{\epsilon}_1, & m \in \mathbb{Z}_{2k}, \\ \epsilon'_0 = -\bar{\epsilon}_0, \end{cases} \quad (2.3)$$

then P_ϵ and $P_{\epsilon'}$ are conjugate under the change $(z, t) \mapsto (\sigma(z), -t)$

(2) In particular, when $\epsilon_0 \in i\mathbb{R}$ and $\arg(\epsilon_1) = -\frac{\pi}{2} - \frac{2m+1}{2k}\pi$, $m \in \mathbb{Z}_{2k}$, then the system is reversible with respect to the line $e^{\frac{2m+1}{2k}\pi i}\mathbb{R}$, i.e. invariant under $(z, t) \mapsto (\sigma(z), -t)$.

Proof. — For real t , the reflection $\sigma : z \mapsto Z = e^{\frac{2m+1}{k}\pi i}\bar{z}$ and the time reversal $t \mapsto T = -t$ sends the vector field (1.5) to

$$\frac{dZ}{dT} = Z(Z^k - \bar{\epsilon}_1 e^{-\frac{2m+1}{k}\pi i} Z - \bar{\epsilon}_0). \quad \square$$

2.3. The conic structure of the bifurcation diagram and normalizations

The bifurcation diagram of the real phase portrait of (1.5) has a conic structure provided by the rescaling (2.1) for $A \in \mathbb{R}^+$. It is therefore sufficient to describe its intersection with a sphere $\mathbb{S}^3 = \{\|\epsilon\| = 1\}$, where

$$\|\epsilon\| = \left(\frac{|\epsilon_0|}{k-1}\right)^{\frac{1}{k}} + \left(\frac{|\epsilon_1|}{k}\right)^{\frac{1}{k-1}}. \quad (2.4)$$

If $\epsilon \neq 0$, we can scale z so that $\|\epsilon\| = 1$ in (1.5). Then it is natural to write $|\epsilon_1| = k(1-s)^{k-1}$ and $|\epsilon_0| = (k-1)s^k$, with $s \in [0, 1]$. The sphere $\mathbb{S}^3 = \{\|\epsilon\| = 1\}$ can be parameterized by three real coordinates: one radial coordinate $s \in [0, 1]$, and two angular coordinates, namely the arguments of ϵ_0 and ϵ_1 . But both arguments act on the position of the singular points. Hence we rather choose one angular parameter θ that will control the relative position of singular points, and a second angular parameter α that will be a rotational parameter, namely we write the system in the form:

$$\dot{z} = z\left(z^k - k(1-s)^{k-1}e^{-i(k-1)\alpha}z + (k-1)s^k e^{i(\theta-k\alpha)}\right). \quad (2.5)$$

This corresponds to

$$\epsilon_0 = (k-1)s^k e^{i(\theta-k\alpha)}, \quad \epsilon_1 = -k(1-s)^{k-1}e^{-i(k-1)\alpha}, \quad \|\epsilon\| = 1, \quad (2.6)$$

with $\theta, \alpha \in [0, 2\pi]$. For all parameter values the system has a singular point at $z_0 = 0$. The two extreme values $s = 0$ and $s = 1$ correspond to the 1-parameter vector fields $\dot{z} = z(z^k + \epsilon_1 z)$ and $\dot{z} = z(z^k + \epsilon_0)$. In the latter there are k singular points at the vertices of a regular k -gon and one singular point at the origin, while in the former there are $k-1$ singular points at

the vertices of a regular $(k - 1)$ -gon and a double singular point at the origin. Moving s from 0 to 1 is the transition from one to the other. The singular point z_0 is double when $\epsilon_0 = 0$, corresponding to $s = 0$ because it has merged with an extra singular point z_1 . The parameter s controls the migration of z_1 outwards when moving from $\epsilon_0 = 0$ to $\epsilon_1 = 0$. When s increases, the movement of the outer singular points z_2, \dots, z_k is very smooth so as to create the exact needed space for the inner singular point z_1 moving outwards. The parameter θ determines the direction in which z_1 moves outwards. The parameter α is a rotation parameter. It plays no role in the relative position of the singular points (these rotate as a rigid solid). On the other hand, it is responsible for the monotonic movements of the separatrices of the pole at infinity producing the bifurcations of homoclinic loops.

Using s and θ as polar coordinates, we will describe the dynamics over the parameter disk $|se^{i\theta}| \leq 1$.

2.4. Geometry of the parameter space

The parameter space is the 3-sphere $\mathbb{S}^3 = \{\|\epsilon\| = 1\}$, which is a quotient of $[0, 1] \times (\mathbb{S}^1)^2$, on which we use coordinates (s, θ, α) defined in (2.6). The quotient consists in identifying

$$\begin{aligned} (s, \theta, \alpha) &\sim (s, \theta + 2\pi, \alpha) \sim (s, \theta, \alpha + 2\pi) \sim (s, \theta + \frac{2\pi}{k-1}, \alpha + \frac{2\pi}{k-1}), \\ (0, \theta, \alpha) &\sim (0, 0, \alpha) \sim (0, 0, \alpha + \frac{2\pi}{k-1}), \\ (1, \theta, \alpha) &\sim (1, 0, \alpha - \frac{\theta}{k}) \sim (1, 0, \alpha - \frac{\theta}{k} + \frac{2\pi}{k}), \end{aligned} \tag{2.7}$$

for all s, θ, α . We naturally find a generalization of the Hopf fibration of \mathbb{S}^3 over \mathbb{S}^2 given by the projection $(s, \theta, \alpha) \mapsto (s, \theta \bmod \frac{2\pi}{k})$, with \mathbb{S}^2 being the quotient of $[0, 1] \times \mathbb{S}^1$ by identifying $(s, \theta) \sim (s, \theta + \frac{2\pi}{k})$ for all s, θ , and $(0, \theta) \sim (0, 0)$, $(1, \theta) \sim (1, 0)$ for all θ . Here $s \in (0, 1)$ parametrizes a family of tori in \mathbb{S}^3 , where each torus is filled by a family of $(k, k - 1)$ -torus knots, each knot corresponding to constant $(s, \theta) = (s_0, \theta_0)$ and being parametrized by α . For $s = 0$, the torus degenerates to a circle parametrized by α and covered $k - 1$ times, and for $s = 1$, the torus degenerates to a circle parameterized by α and covered k times.

The only bifurcations are homoclinic connections of two separatrices of ∞ , and the two bifurcations of parabolic point. The former, of real codimension 1, is studied through the periodgon. Several bifurcations can occur simultaneously, yielding higher order bifurcations. The boundaries of the surfaces of homoclinic connections in parameter space occur along the higher order bifurcations, including the parabolic point bifurcations.

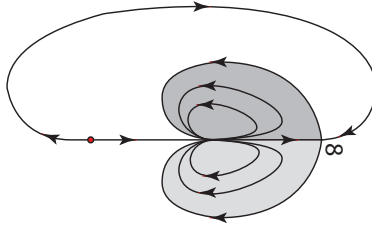


Figure 2.1. The two sepal zones of the parabolic point of $\dot{z} = z^3 + z^2$.

2.5. Bifurcation of parabolic points

Parabolic points are important because they organize the dynamics and the bifurcations of homoclinic loops. A parabolic point of codimension ℓ has 2ℓ *sepal zones*, i.e. connected regions filled by trajectories having their α -limit and ω -limit at the parabolic point. These sepal zones go to ∞ . Generically each sepal zone coincides with a saddle sector of ∞ , called a *sepal sector* of ∞ (see Figure 2.1 and Figure 2.2, except (b) and (f)). Exceptionally, a sepal zone can have homoclinic loops in its boundary as in Figure 2.2(b) and (f). The sepal zones are bounded by separatrices of infinity. Generically, the boundary of a sepal zone is the limit of a homoclinic loop through ∞ that circles around a unique singular point. Exceptionally the boundary can be the limit of several homoclinic loops (Figure 2.2(b) and (f)).

PROPOSITION 2.3.

(1) *There are two kinds of bifurcations of parabolic point of codimension 1.*

- *Bifurcation of parabolic point at the origin when $\epsilon_0 = 0$ (see Figure 2.2). The two sepal zones at the parabolic point correspond to two almost opposite sepal sectors at ∞ , namely if m_1 and m_2 are the number of adjacent non sepal sectors between the two sepal sectors, then m_1 and m_2 are even and $|m_1 - m_2| \leq 2$.*
- *The other type occurs when the discriminant of $z^k + \epsilon_1 z + \epsilon_0$ vanishes and $\epsilon_0, \epsilon_1 \neq 0$. The discriminant is given by*

$$\Delta(\epsilon_1, \epsilon_0) = (-1)^{\lfloor \frac{k}{2} \rfloor} (k-1)^{k-1} k^k \left[\left(\frac{\epsilon_0}{k-1} \right)^{k-1} - \left(-\frac{\epsilon_1}{k} \right)^k \right]. \quad (2.8)$$

The intersection of $\Delta = 0$ with the sphere \mathbb{S}^3 is a $(k, k-1)$ torus knot. Using (2.6), Δ vanishes if and only if $s = \frac{1}{2}$ and $\theta = \frac{2\pi j}{k-1}$, in which case $z = \frac{1}{2} e^{\frac{2\pi j}{k-1}}$ is a generic parabolic point (double root) of (1.5) (see Figure 2.3). The two sepal zones

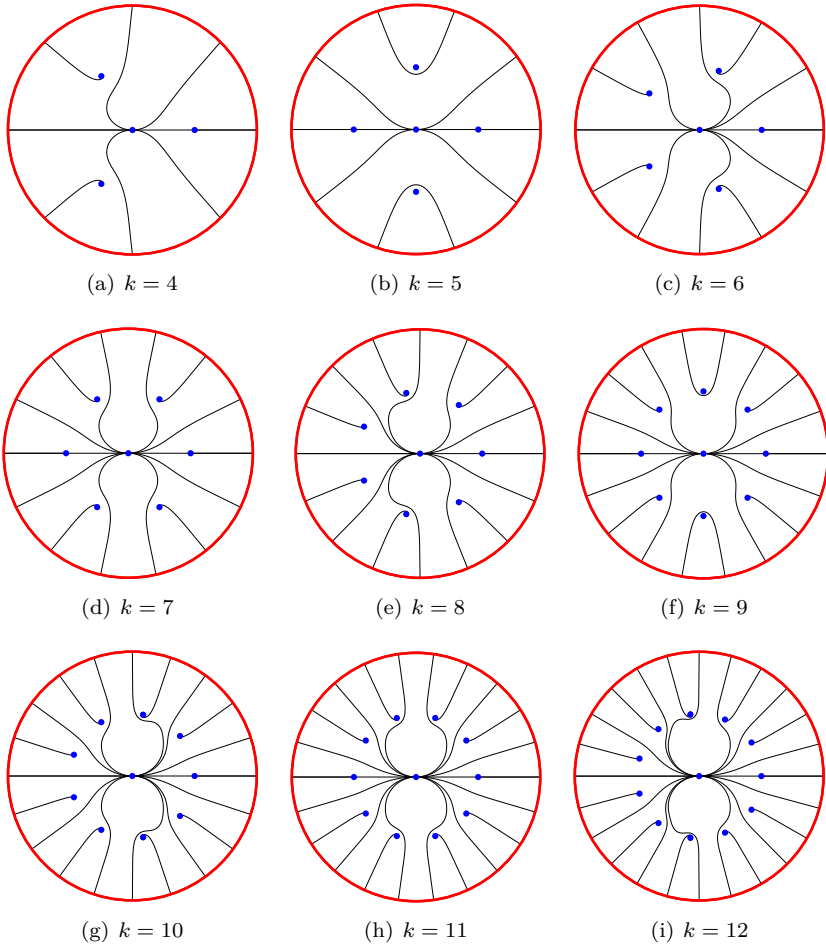


Figure 2.2. The phase portrait of $\dot{z} = z^{k+1} - z^2$ with a parabolic point of codimension 1 at the origin.

at the parabolic point correspond to two adjacent sepal sectors at ∞ .

- (2) *A bifurcation of parabolic point of codimension k occurs when $\epsilon_0 = \epsilon_1 = 0$, in which case the origin is a singular point of multiplicity $k + 1$.*

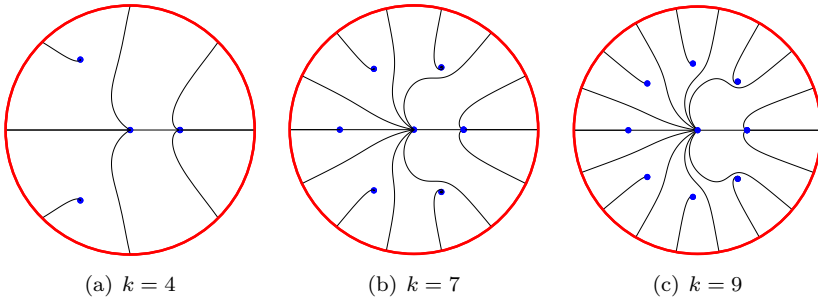


Figure 2.3. The phase portrait of $\dot{z} = z^{k+1} - kz^2 + (k-1)z$ with a parabolic point of codimension 1 at $z = 1$.

3. The periodgon of (1.5)

3.1. The definition of the periodgon of a polynomial vector field

Let $\dot{z} = \frac{dz}{dt} = P(z)$ be a polynomial vector field of degree $k + 1$ with singular points z_0, \dots, z_k and

$$\nu_j = 2\pi i \operatorname{Res}_{z_j} \frac{1}{P(z)}$$

be the period of z_j : this period corresponds to the “travel time” $\int_{\gamma_j} dt$ along a small loop γ_j surrounding only z_j . If z_j is simple, then $\nu_j = \frac{2\pi i}{P'(z_j)}$. Note that any simple equilibrium point z_j is a center of the rotated vector field

$$\dot{z} = e^{i \arg \nu_j} P(z). \quad (3.1)$$

DEFINITION 3.1. — *Let $\dot{z} = \frac{dz}{dt} = P(z)$ be a polynomial vector field and z_j be a simple singular point. The periodic domain of z_j is the basin of the center (periodic zone) at z_j of (3.1). The boundary of the periodic domain of z_j consists in one or several homoclinic loops through the pole at infinity of (3.1), which are called the homoclinic loop(s) of z_j .*

LEMMA 3.2 ([4]). — *When all singular points of a vector field $\dot{z} = \frac{dz}{dt} = P(z)$ are simple, then their periodic domains are disjoint. If, moreover, they have only one homoclinic loop, then these homoclinic loops are disjoint. If some points have multiple homoclinic loops, then some homoclinic loops agree up to orientation.*

This lemma allows defining the periodgon in the generic case where all singular points have exactly one homoclinic loop. The periodgon lies in the

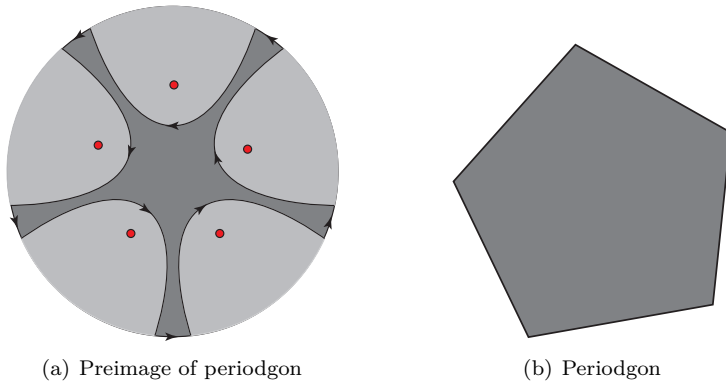


Figure 3.1. The periodgon in t -space and its preimage in z -space.

time-space t , a translation surface, where

$$t = \int \frac{dz}{P(z)}.$$

The variable t is well defined in the translation surface up to a translation as long as the variable z is restricted to a simply connected domain of \mathbb{C} containing no singular points.

DEFINITION 3.3. — *Let $\dot{z} = \frac{dz}{dt} = P(z)$ be a polynomial vector field with simple singular points, each having exactly one homoclinic loop. Then the periodgon of the vector field is the image in t -space of the complement of the union of the periodic domains bounded by the homoclinic loops (see Figure 3.1). This definition has a limit in the nongeneric case where some singular point has more than one homoclinic loop (see Figures 3.2 and 3.3). But the order of the sides in the nongeneric case is not uniquely defined, this coming from the fact that different generic situations have the same limit.*

3.2. The periodgon in the degenerate case

It is possible to generalize the notion of periodgon in the degenerate case when some singular point is parabolic (see [4]). For that, we need to define the parabolic domain of a parabolic point.

DEFINITION 3.4.

- (1) *A sepal zone of a parabolic point is a connected component of the complement of the union of the separatrices, which is filled by trajectories having their α -limit and ω -limit at the parabolic point.*

Two-parameter unfolding of a parabolic point

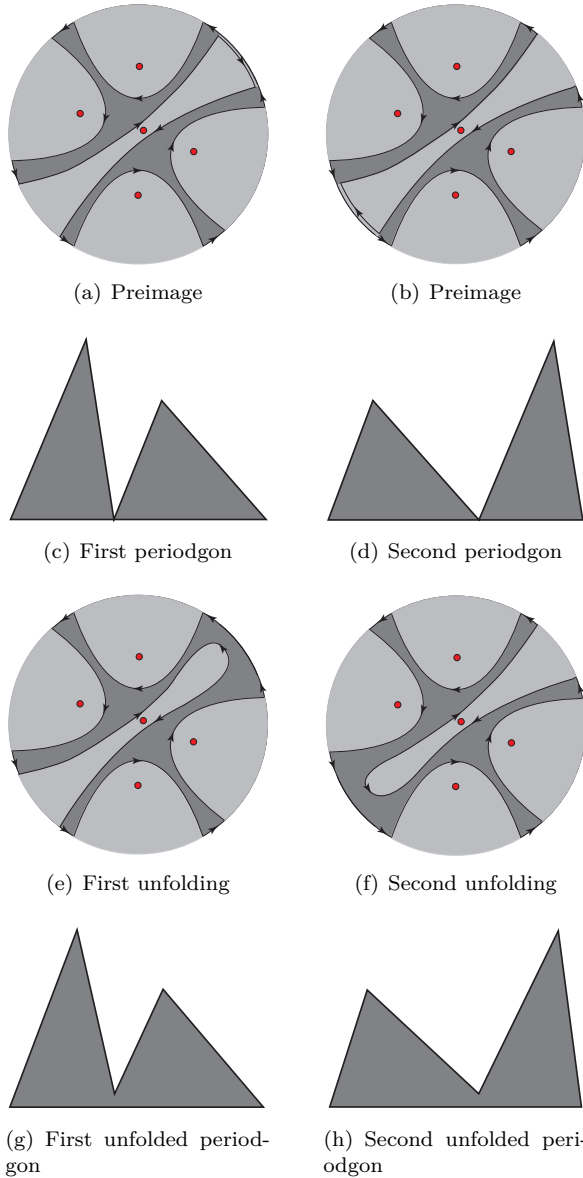


Figure 3.2. The same preimage ((a) and (b)) in z -space corresponds to two different nongeneric periodgons in (c) and (d). The respective unfoldings of the preimages appear in (e) and (f) and their corresponding unfolded periodgons in (g) and (h).

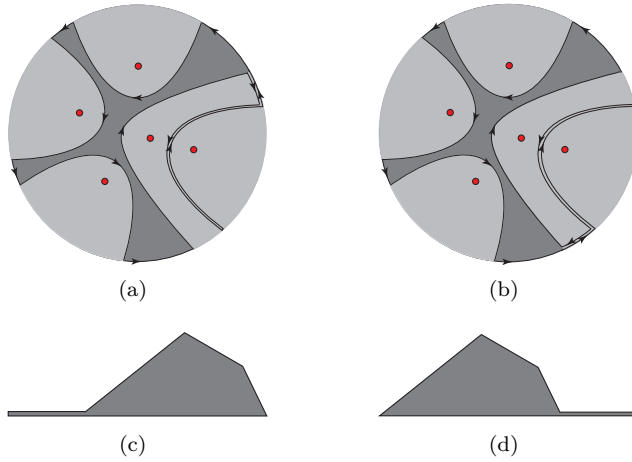


Figure 3.3. In (a) and (b), another preimage in z -space corresponding to two different nongeneric periodgons in (c) and (d). The unfoldings are not drawn.

- (2) *The parabolic domain of a parabolic point z_0 of a polynomial vector field $\dot{z} = P(z)$ is the union of all sepal zones of z_0 in all rotated vector fields $e^{i\beta}P(z)$ (see Figures 3.4 and 3.5).*
- (3) *The boundaries of the periodic and parabolic domains of the different singular points intersect only at infinity (except when they share a homoclinic loop) and the periodgon is the image in t -space of the complement of the union of the periodic and parabolic domains.*

Note that the periodgon has no limit when approaching a parabolic point. Indeed, two sides of the periodgon become infinite. Moreover, their argument makes a nearly full turn (resp. a nearly half-turn full) around the origin when considering an unfolding of the form $\dot{z} = z^2 - \epsilon z + O(z^3)$ (resp. $\dot{z} = z^2 - \epsilon + O(z^3)$) (see Figure 3.6).

3.3. The rotational property with respect to α

The change of coordinate $z \mapsto Z = e^{i\alpha}z$ brings (2.5) to the form

$$\dot{Z} = e^{-ik\alpha}Z (Z^k - k(1-s)^{k-1}Z + (k-1)s^k e^{i\theta}).$$

The periodgon of (2.5) is that of $\dot{Z} = Z (Z^k - k(1-s)^{k-1}Z + (k-1)s^k e^{i\theta})$ rotated by $e^{-ik\alpha}$. Hence, it suffices to study the shape of the periodgon for $\alpha = 0$.

Two-parameter unfolding of a parabolic point

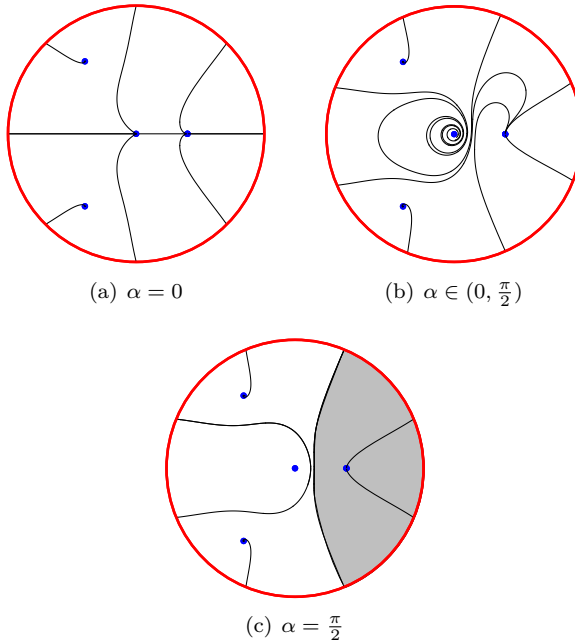


Figure 3.4. The phase portrait of $\dot{z} = e^{i\alpha}(z^5 - 4z^2 + 3z)$ with a parabolic point at $z = 1$ and the parabolic domain in (c).

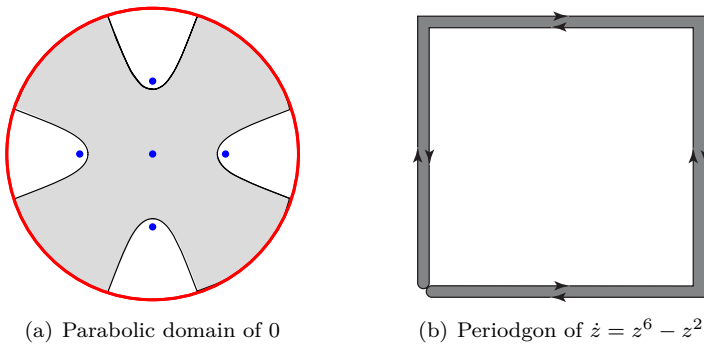


Figure 3.5. The parabolic domain of the origin in $\dot{z} = z^6 - z^2$. Since the parabolic domain is the complement of the union of the periodic domains of the four singular points, then the periodgon has empty interior in this case.

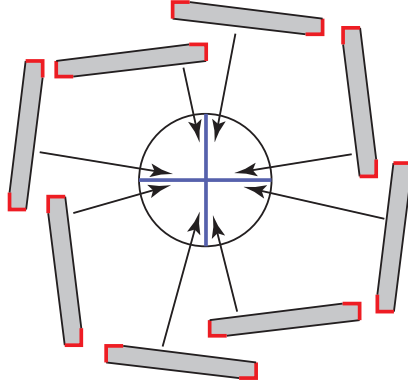


Figure 3.6. The bifurcation diagram of the periodgon of $\dot{z} = z^6 - z^2 + se^{i\theta}z$ for s small. The center circle is the parameter space $se^{i\theta}$ for s small and $\theta \in [0, 2\pi]$. The lengths of the black sides, corresponding to the periods of z_0 and z_1 , tend to infinity when $s \rightarrow 0$. The bifurcations occur for $\theta = \frac{m\pi}{2}$.

3.4. The eigenvalues of (1.5)

Because of all the symmetries described in Section 2.2 we limit ourselves to $\theta \in (0, \frac{\pi}{k-1})$ and, as discussed in Section 3.3, to $\alpha = 0$. We are interested in understanding the shape of the periodgon. Let us call $z_0 = 0$, and let z_1, \dots, z_k be the other singular points. They are numbered by increasing argument starting with z_1 , where $\arg(z_1) \in (\theta, \frac{\pi-\theta}{k})$. Let λ_j be the eigenvalue of z_j . Then,

$$\begin{cases} \lambda_0 = (k-1)s^k e^{i\theta}, \\ \lambda_j = k(k-1)((1-s)^{k-1}z_j - s^k e^{i\theta}), \quad j = 1, \dots, k. \end{cases} \quad (3.2)$$

LEMMA 3.5. — For $s \neq 0, 1$, the eigenvalue λ_0 can only be collinear with one of the λ_j if $\theta = \frac{\pi\ell}{k-1}$ for some integer ℓ .

Proof. — If λ_j is collinear with λ_0 and $s \neq 0, 1$, then (3.2) implies that $\arg z_j = \theta + m_1\pi$ for some integer m_1 . This in turn implies that $\arg z_j^k = \theta + m_2\pi$, for some integer m_2 , hence the result. \square

LEMMA 3.6. — For all $s > 0$ and $\theta \in [0, \frac{\pi}{k-1}]$, then $\text{Re}(\lambda_0) > 0$, and $\text{Re}(\lambda_j) < 0$ if $\text{Re}(z_j) < 0$ and $j > 0$. For s close to 1, then $\text{Re}(\lambda_j) < 0$ for all $j > 0$. Moreover, if $\text{Re}(z_j) > 0$ for all s , then $\text{Re}(\lambda_j)$ changes sign when s decreases from 1 to 0.

Proof. — This follows from (3.2). \square

3.5. Preliminaries on the singular points

Since for $\alpha = 0$ the singular points apart from $z_0 = 0$ are the same as those of $\dot{z} = z^k - k(1-s)^{k-1}z + (k-1)s^k e^{i\theta}$ we can apply the results of [4].

PROPOSITION 3.7 ([4]). — *We consider (2.5) with $\theta \in [0, \frac{\pi}{k-1}]$ and $s \in [0, 1]$. Let $z_0 = 0$, and z_1, \dots, z_k be the other singular points.*

- (1) *The singular points $z_1(s, \theta, 0), \dots, z_k(s, \theta, 0)$ have distinct arguments for all $s \in (0, 1]$, unless $\theta = 0$, in which case the two roots $z_1(s, 0, 0)$ and $z_k(s, 0, 0)$ both have zero argument for $s \leq \frac{1}{2}$. Then it makes sense ordering them by increasing value of argument. (When $s = 0$, then z_2, \dots, z_k have distinct arguments.)*
- (2) *If $z_j(s, \theta, 0) \notin e^{i\theta}\mathbb{R}$, then the absolute value of $\arg(e^{-i\theta}z_j(s, \theta, 0)) \in (-\pi, \pi)$ increases monotonically with s .*
- (3) *This implies that*

$$z_1(0, \theta, 0) = 0, \quad \text{and} \quad z_j(0, \theta, 0) = k^{\frac{1}{k-1}} e^{\frac{2\pi i(j-1)}{k-1}}, \quad j = 2, \dots, k,$$

and the roots are caught for all $s \in [0, 1]$ in the following disjoint sectors:

$$\arg z_1(s, \theta, 0) \in \left[\theta, \frac{\theta + \pi}{k} \right],$$

$$\arg z_j(s, \theta, 0) \in \left[\frac{2\pi(j-1)}{k-1}, \frac{\theta + (2j-1)\pi}{k} \right], \quad \text{for } 2 \leq j \leq \frac{k+1}{2},$$

$$\arg z_j(s, \theta, 0) \in \left[\frac{\theta + (2j-1)\pi}{k}, \frac{2\pi(j-1)}{k-1} \right], \quad \text{for } \frac{k}{2} + 1 \leq j \leq k.$$

- (4) *For $\theta = 0$, the two roots $z_1(s, 0, 0)$ and $z_k(s, 0, 0)$ are real for $s \in [0, \frac{1}{2}]$ and merge for $s = \frac{1}{2}$. For $s > \frac{1}{2}$, they split apart in the imaginary direction.*

LEMMA 3.8. — *We consider (2.5) with $\alpha = 0$, $\theta \in [0, \frac{\pi}{k-1}]$ and $s \in [0, 1]$. Let $z_0 = 0$, and z_1, \dots, z_k be the other singular points. Then two distinct nonzero roots z_j and z_ℓ , $j, \ell > 0$, cannot point in opposite directions unless $\theta = 0$ or $\theta = \frac{\pi}{k-1}$.*

Proof. — Suppose that $z_j = r_j e^{i\phi}$ and $z_\ell = -r_\ell e^{i\phi}$. Then $(r_j^k - (-1)^k r_\ell^k) \times e^{i(k-1)\phi} - k(1-s)^{k-1}(r_j + r_\ell) = 0$, from which it follows that $e^{i(k-1)\phi} = \pm 1$. Substituting into $z^k - k(1-s)^{k-1}z + (k-1)s^k e^{i\theta} = 0$ yields the result. \square

3.6. Shape of the periodgon

To understand the shape of the periodgon we need to understand the boundaries of the periodic domains of the singular points. We conjecture

that the boundaries of the periodic domains of the z_j for $j > 1$ always consist of a single homoclinic loop: this is supported by numerical simulations. It is only the boundaries of the periodic domains of z_0 and z_1 which undergo several bifurcations when the parameters vary. This is what we study now. We start with the situations $s = 0$ and $s = 1$, and then vary $s \in (0, 1)$. All these are steps to prove the following theorem

THEOREM 3.9.

- (1) *The boundary of the periodic domain of z_0 has more than one homoclinic loop for*

$$\begin{cases} \theta = \frac{2j\pi}{k-1}, & k \text{ odd, and } s \in (0, 1), \\ \theta = \frac{(2j-1)\pi}{k-1}, & k \text{ even, and } s \in (0, 1). \end{cases}$$

The boundary of the periodic domain of z_1 has more than one homoclinic loop for

$$\theta = \frac{2j\pi}{k-1}, \quad \text{all } k, \text{ and } s \in \left(0, \frac{1}{2}\right).$$

- (2) *There are no other bifurcations of the periodgon*

- *In the neighborhood of $s = 0$;*
- *In the neighborhood of $s = 1$;*
- *In the neighborhood of $\theta = \frac{2j\pi}{k-1}$, $j = 0, \dots, k-2$;*
- *For even k , in the neighborhood of $\theta = \frac{(2j-1)\pi}{k-1}$, $j = 0, \dots, k-2$.*

This leads to the conjecture.

CONJECTURE 3.10. — *The only bifurcations of the periodgon occur*

- *along the rays $\theta = \frac{2j\pi}{k-1}$ for k odd;*
- *along the rays $\theta = \frac{(2j-1)\pi}{k-1}$ and the half-rays $\theta = \frac{2j\pi}{k-1}$, $s \in (0, \frac{1}{2})$ for k even.*

Moreover, only the singular points z_0 and z_1 can have more than one homoclinic loop.

3.6.1. Proof of Theorem 3.9

We discuss here (1) and (2) simultaneously. Indeed, (2) follows from transversality properties for the situations studied in (1).

Two-parameter unfolding of a parabolic point

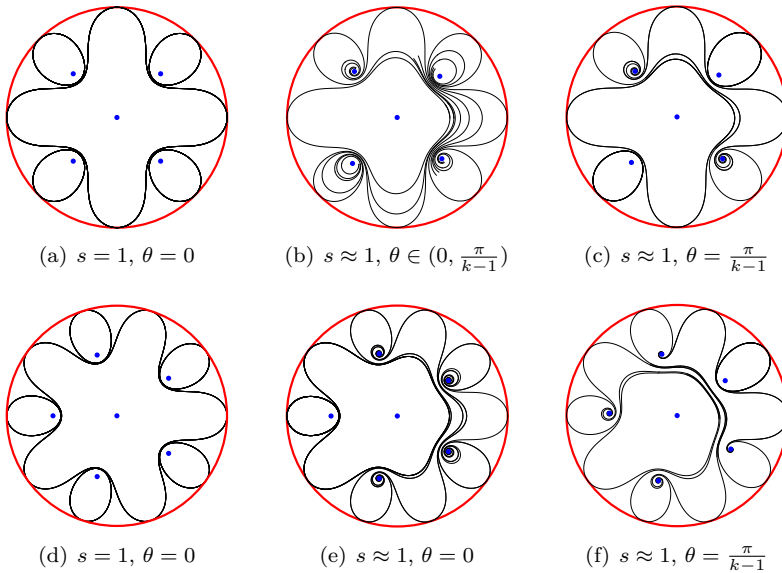


Figure 3.7. The boundary of the periodic domain (homoclinic loop(s)) of z_0 for $s \approx 1$, $\alpha = \frac{\theta}{k}$ and $k = 4$ (resp. $k = 5$) on the upper (resp. lower) row. The figures are obtained by integrating on a disk the vector field $\dot{z} = e^{i\delta} P_\epsilon'(z)$ so that $e^{i\delta} P_\epsilon'(z_0) \in i\mathbb{R}$. We see multiple homoclinic loops around z_0 for $\theta = 0$, k odd and $\theta = \frac{\pi}{k-1}$, k even.

The case $s = 1$. — Using the change $z \mapsto Z = e^{-i\frac{\theta}{k}} z$ it suffices to study the boundary of the periodic domain of z_0 from the system $\dot{Z} = iZ(Z^k + k)$, for which all points are simultaneously centers. Moreover, the system is symmetric under $z \mapsto e^{i\frac{2\pi}{k}} z$, and hence so is the boundary of the periodic domain of z_0 . Then it consists of k homoclinic loops as in Figure 3.7(a) and (d). The periodgon in that case is degenerate to a long line segment corresponding to the vector ν_0 and k small segments corresponding to vectors $\nu_j = -\frac{\nu_0}{k}$, $j > 0$.

The case $s = 0$. — Here $z_0 = z_1$ is a parabolic point. In the case of one parabolic point the periodgon has been defined in Section 3.2, but it is not the limit when $s \rightarrow 0$ of the periodgon for $s \neq 0$. However, to understand the periodgon for s small we need to understand the periodic domains at $s = 0$ of the nonzero singular points, and which separatrices of ∞ land at z_0 . Looking at the system $\dot{z} = z^2(z^{k-1} - k)$, then $\lambda_j = k(k-1)z_j$ for $j \geq 2$, from which it follows that each $\text{Re}(\lambda_j)$ has the sign of $\text{Re}(z_j)$. This allows drawing the phase portrait (see Figure 2.2). Indeed, the sepal zones of the

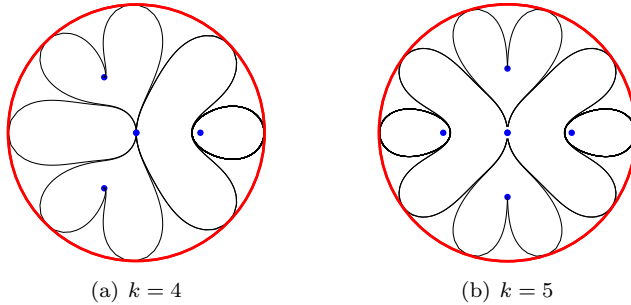


Figure 3.8. The phase portrait of $\dot{z} = i(z^{k+1} - kz^2)$.

parabolic point separate the singular points into two groups: the attractive ones on one side, and the repelling ones on the other side. There are also two centers when $k \equiv 1 \pmod{4}$: the basin of each center is surrounded by a sepal zone.

The nonzero singular points are of the form $z_j = \exp\left(\frac{2\pi(j-1)}{k-1}i\right)$, $j = 2, \dots, k$, with eigenvalues given in (3.2). Now, consider the system $\dot{z} = iP_\epsilon(z)$, which is reversible with respect to the real axis. There are one (resp. two) additional singular points on the real axis for k even (resp. k odd), which are centers. The singular points in the upper (resp. lower) half-plane are attracting (resp. repelling) for $s = 0$, and that remains the case for s small. This yields the phase portraits in Figure 3.8 for the vector field $\dot{z} = iP_\epsilon(z)$, since all attracting (resp. repelling) singular points are necessarily linked to the repelling (resp. attracting) sector of the parabolic point at $s = 0$.

The case $\theta = \frac{2j\pi}{k-1}$. — (See Figures 3.7(e) and 3.9(a) and (d).) It suffices to consider the case $\theta = 0$, where the system is symmetric with respect to the real axis. For $s \in (0, \frac{1}{2})$ and $\theta = 0$, the system has 3 (resp. 4) singular points on the real axis for k even (resp. odd), and they are simultaneously centers of the system $\dot{z} = iP_\epsilon(z)$. Then $0 = z_0 < z_1 < z_k$, from which it follows that the periodic domain of z_1 is bounded by two homoclinic loops. When $s = \frac{1}{2}$, the points z_1 and z_k merge in a parabolic point. Then z_1 (resp. z_k) moves in the upper (resp. lower) half-plane for $s > \frac{1}{2}$. Hence, the periodic domain of z_1 is between those of z_2 and z_k and this is also valid for small θ . Similarly for odd k we have $z_{\frac{k+1}{2}} < z_0 = 0$, yielding that z_0 has two homoclinic loops. For small positive θ , then the periodic domain of z_0 is between that of $z_{\lfloor \frac{k+1}{2} \rfloor}$ and that of $z_{\lceil \frac{k}{2} \rceil + 1}$. From (3.2), the singular point z_j , $j \geq 2$, of system $\dot{z} = iP_\epsilon(z)$ is attracting (resp. repelling) if $\text{Im}(z_j) > 0$ (resp. $\text{Im}(z_j) < 0$). Hence, from the symmetry, the singular points not on

the real axis are linked two by two and the passage for these links is to the right of z_0 .

The case $\theta = \frac{(2j-1)\pi}{k-1}$. — (See Figures 3.7(c) and (f) and 3.9(c) and (f).)

It suffices to consider the case $j = 1$. The change $Z = e^{-i\frac{\pi}{k-1}}z$ transforms the system into $\dot{Z} = e^{-i\frac{\pi}{k-1}}Z(-Z^k - k(1-s)^{k-1}Z + (k-1)s^k)$, which means that the periodic domains of the singular points along the axis $Z = 0$ can be seen from the system

$$\dot{Z} = \omega(Z) = iZ(-Z^k - k(1-s)^{k-1}Z + (k-1)s^k),$$

again a reversible system with respect to the real axis. For k even there is always a singular point $Z_{\frac{k}{2}+1}$ on \mathbb{R}^- , whose homoclinic loop is part of the boundary of the periodic domain of $z_0 = Z_0 = 0$. Hence, there is always a bifurcation of the periodgon along the line $\theta = \frac{(2j-1)\pi}{k-1}$ for k even. The eigenvalue at the singular point Z_j of $\dot{Z} = \omega(Z)$ is again of the form $i\lambda_j$ for λ_j defined in (3.2) (with z_j replaced by Z_j). Hence Z_j is attracting (resp. repelling) if $\text{Im}(Z_j) > 0$ (resp. $\text{Im}(Z_j) < 0$). As in the case for $\theta = 0$, each singular point of the upper half-plane is linked to one in the lower half-plane and the passage is between Z_0 and Z_1 . Hence (modulo the conjecture that the Z_j , $j \geq 2$, always have a unique homoclinic loop,) there is no bifurcation of the periodgon for increasing $s \in (0, 1)$, and the order of the sides is the same as the one for s small, which will be discussed below.

The case s close to 1. — We start by computing the eigenvalues for $\alpha = \frac{\theta}{k}$. Let λ_j be the eigenvalue of z_j . Then,

$$\begin{cases} \lambda_0 = (k-1)s^k, \\ \lambda_j = k(k-1) \left((1-s)^{k-1} e^{-i\frac{(k-1)\theta}{k}} z_j - s^k \right), \quad j = 1, \dots, k. \end{cases} \quad (3.3)$$

To compute the boundary of the periodic domain of z_0 we multiply the system and its eigenvalues by i . Then $\text{Re}(i\lambda_j) > 0$ if and only if $\text{Im}(\lambda_j) < 0$, and $\text{Im}(\lambda_j)$ has the sign of $\text{Im}(e^{-i\frac{(k-1)\theta}{k}} z_j)$. For $s = 1$, then $z_j = (k-1)^{\frac{1}{k}} \times e^{i\frac{(2j-1)\pi}{k}}$. Hence

$$\text{Im}(\lambda_j) \begin{cases} > 0, & 1 \leq j \leq \frac{k}{2}, \\ < 0, & \frac{k+1}{2} < j \leq k, \\ < 0 & j = \frac{k+1}{2}, \theta > 0, \quad k \text{ odd}, \\ = 0, & j = \frac{k+1}{2}, \theta = 0, \quad k \text{ odd}. \end{cases}$$

This gives the direction in which the homoclinic loops that surround all singular points z_j , $j > 0$, are broken in $\dot{z} = iP_\epsilon(z)$ for s close to 1. Indeed, for $s = 1$, all singular points are centers. When $s \neq 1$, the point z_j becomes an attracting (resp. repelling) focus when $\text{Im}(\lambda_j) > 0$ (resp. negative), and remains a center when $\text{Im}(\lambda_j) = 0$. Since the vector field can have no limit

cycle, this gives the direction in which the homoclinic loop is broken. Of course, since everything is continuous, it suffices to see how it is broken for $\theta = 0$, which has been studied above. The case $\alpha = 0$ comes by applying the change of variable $z \mapsto Z = e^{i\alpha}z$ as described in Section 3.3. The factor $e^{-ik\alpha}$ has no influence on the shape of the periodic domains. Hence the periodic domains for $\alpha = 0$ are obtained by rotating those for $\alpha = \frac{\theta}{k}$ of an angle $\alpha = \frac{\theta}{k} \in [0, \frac{\pi}{k(k-1)}]$.

The case s close to 0. — Here we consider the case $\alpha = 0$.

For $s = 0$, let us first compute the periodic domain of $z_j = k^{\frac{1}{k-1}} \exp(\frac{2\pi j i}{k-1})$, $j \geq 2$. It is the domain of the center at z_j for $\dot{z} = i \exp(-\frac{2\pi j i}{k-1})(z^{k+1} - kz^2)$. Letting $Z = \exp(-\frac{2\pi j i}{k-1})z$ changes the system to $\dot{Z} = iZ^2(Z^{k-1} - k)$, whose phase portrait appears in Figure 3.8. Because of the symmetry and the fact that $Z_j \in \mathbb{R}^+$, this shows that its periodic domain is bounded by a unique homoclinic loop.

For $s \approx 0$, the boundary of the periodic domain (homoclinic loop(s)) of z_0 for different values of $\theta \in [0, \frac{\pi}{k-1}]$ and that of z_1 for $\theta \in \{0, \frac{\pi}{k-1}\}$ appear in Figure 3.9. This comes from the knowledge at $s = 0$, at $\theta = 0$ and $\theta = \frac{\pi}{k-1}$, as studied above.

For $\theta \in (0, \frac{\pi}{k-1})$, the symmetry existing for $\theta = 0$ is broken, and all periodic domains have one homoclinic loop. To find the periodic domain of z_0 we must now consider the vector field $\dot{z} = e^{i(\frac{\pi}{2}-\theta)}P_\epsilon(z)$. The points that were previously on the real axis are $z_k = k^{\frac{1}{k-1}}(1-s) - k^{-1}s^k e^{i\theta} + o(s^k)$ and, for k odd, $z_{\frac{k+1}{2}} = -k^{\frac{1}{k-1}}(1-s) - k^{-1}s^k e^{i\theta} + o(s^k)$, yielding that $\text{Re}(e^{i(\frac{\pi}{2}-\theta)}\lambda_k) > 0$ (resp. $\text{Re}(e^{i(\frac{\pi}{2}-\theta)}\lambda_{\frac{k+1}{2}}) < 0$ for k odd). Then z_k (resp. $z_{\frac{k+1}{2}}$ for k odd) is a repelling (resp. attracting) point of $\dot{z} = e^{i(\frac{\pi}{2}-\theta)}P_\epsilon(z)$.

Hence, the periodic domain of z_0 is between that of $z_{\lfloor \frac{k+1}{2} \rfloor}$ and that of $z_{\lceil \frac{k}{2} \rceil + 1}$, while that z_1 is between z_k and z_2 .

The case $s \approx \frac{1}{2}$ and $\theta \approx 0$. — There is a parabolic point with $z_1 = z_k$ for $(s, \theta) = (\frac{1}{2}, 0)$. What happens here is very close to the situation studied in [4], where the periodic domain of z_1 is bounded by two homoclinic loops for real $s < \frac{1}{2}$ and by one homoclinic loop elsewhere.

This ends the proof of Theorem 3.9. □

3.6.2. Discussion of Conjecture 3.10

The conjecture is motivated by the fact that the proposed bifurcation diagram for the periodgon is the simplest that connects the known bifurcations.

Two-parameter unfolding of a parabolic point

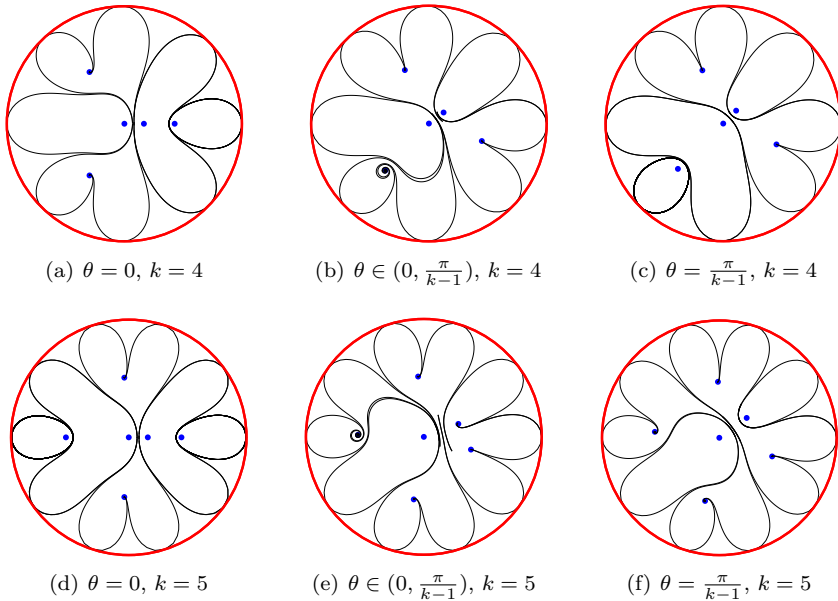


Figure 3.9. For $s \approx 0$, the boundary of the periodic domain (homoclinic loop(s)) of z_0 for different values of $\theta \in [0, \frac{\pi}{k-1}]$ and that of z_1 for $\theta \in \{0, \frac{\pi}{k-1}\}$. The figures are obtained by integrating on a disk $\dot{z} = e^{i\delta}P_\epsilon(z)$ so that $e^{i\delta}P'_\epsilon(z_0) \in i\mathbb{R}$. We see multiple homoclinic loops around z_1 for $\theta = 0$, and around z_0 for $\theta = 0, k$ odd and $\theta = \frac{\pi}{k-1}, k$ even.

Moreover, the numerical simulations show no bifurcations of the periodgon outside these bifurcation loci. See for instance Figures 3.10 and 3.11.

4. The bifurcation diagram of (1.5)

THEOREM 4.1. — *The bifurcation diagram of (1.5) consists of*

- (1) *Real codimension 1 bifurcations of homoclinic loops. These occur when exactly two vertices of the periodgon can be joined by a horizontal segment inside the closed periodgon.*
- (2) *Real codimension 2 bifurcations of parabolic points for $\epsilon_0 = 0$ and $\Delta = 0$, where Δ is given in (2.8).*
- (3) *The only bifurcations of higher order are intersections of bifurcations of the two previous types.*

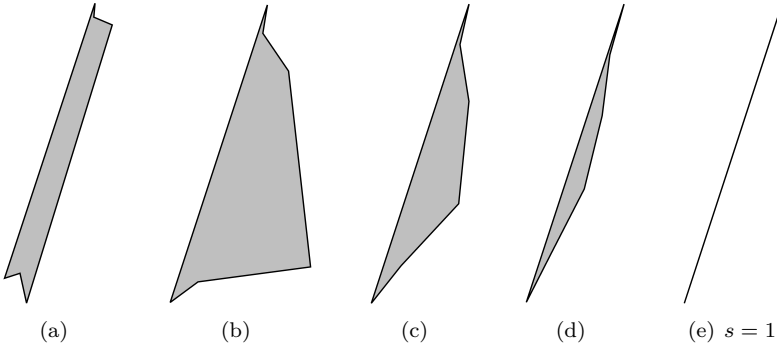


Figure 3.10. The periodgon for $k = 5$, $\theta = \pi/10$ and increasing nonzero values of s .

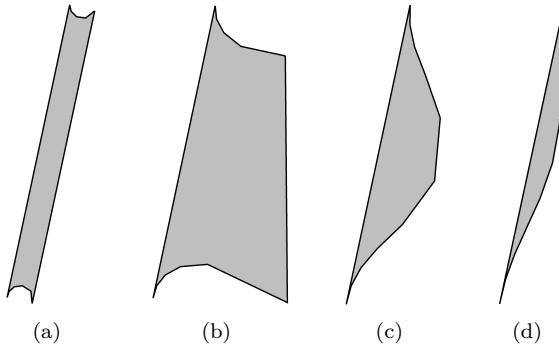


Figure 3.11. The periodgon for $k = 10$, $\theta = \pi/15$ and increasing nonzero values of s .

- (4) All bifurcations occur on hypersurfaces, surfaces or curves invariant under $(\epsilon_1, \epsilon_0) \mapsto (r^{k-1}\epsilon_1, r^k\epsilon_0)$ for $r > 0$.
- (5) On \mathbb{S}^3 , the boundaries of the codimension 1 bifurcation surfaces are either higher order homoclinic loops or pieces of the curves $\epsilon_0 = 0$ and/or $\Delta = 0$.

Remark 4.2. — Under Conjecture 3.10 the periodgon is planar. In the general case, it is a simply connected region of a translation surface. A homoclinic loop occurs precisely when two vertices of the periodgon can be joined by a horizontal segment inside that translation surface.

5. The bifurcation diagram of a generic 2-parameter unfolding of a parabolic point of codimension k preserving the origin

In this section we consider a two-parameter unfolding preserving the origin of a germ of analytic vector field with a parabolic point at the origin, which we can, without loss of generality, suppose to be of the form $\dot{z} = z^{k+1} + Az^{2k+1} + o(z^{2k+1})$. Using the Weierstrass preparation theorem and a scaling in z , such an unfolding has the form $\dot{z} = zQ_\eta(z)(1 + g_\eta(z))$, with $Q_\eta(z) = z^k + \sum_{j=0}^{k-1} b_j(\eta)z^j$ depending on $\eta = (\eta_1, \eta_0) \in (\mathbb{C}^2, 0)$, and $g_\eta(z) = g(\eta, z) = O(z)$. The unfolding is generic if

$$\left| \frac{\partial(b_1, b_0)}{\partial(\eta_1, \eta_0)} \right| \neq 0. \quad (5.1)$$

Dividing $g(z)$ by $zQ_\eta(z)$ allows writing the vector field as

$$\dot{z} = zQ_\eta(z)(1 + R_\eta(z) + zQ_\eta(z)h_\eta(z)) \quad (5.2)$$

where $R_\eta(z) = \sum_{j=1}^k c_j(\eta)z^j$ is such that $c_j(0) = 0$ for $j < k$. We change parameter to $\epsilon = (\epsilon_1, \epsilon_0) = (b_1(\eta), b_0(\eta))$ and we still note the polynomials by Q_ϵ and R_ϵ .

The vector field in the form (5.2) is called *prepared*. In particular the eigenvalues at the singular points $z_0 = 0$ and z_j , $j = 1, \dots, k$, depend only of the polynomials Q_ϵ and R_ϵ . More precisely,

$$\begin{cases} \lambda_0 = \epsilon_0 \\ \lambda_j = z_j Q'_\epsilon(z_j)(1 + R_\epsilon(z_j)). \end{cases} \quad (5.3)$$

Note that $1 + R_\epsilon(z_j)$ is close to 1 for ϵ small.

We want to study the phase portrait of (5.2) for z in some small fixed disk \mathbb{D}_r and all ϵ in a small polydisk $\mathbb{D}_\rho = \{\|\epsilon\| < \rho\}$. By taking a smaller r it is always possible to suppose that the vector field is defined on $\partial\mathbb{D}_r$. The radius r is chosen sufficiently small so that the vector field has the same behavior as $\dot{z} = z^{k+1}$ near $\partial\mathbb{D}_r$ (see Figure 5.1). Similarly, ρ is chosen sufficiently small so that the $k + 1$ singular points bifurcating from the origin remain far from $\partial\mathbb{D}_r$.

The bifurcation diagram has a conic like structure. This is seen by writing the parameters as

$$\epsilon = \left(-k\zeta^{k-1}(1-s)^{k-1}e^{-i(k-1)\alpha}, (k-1)\zeta^k s^k e^{i(\theta-k\alpha)} \right) \quad (5.4)$$

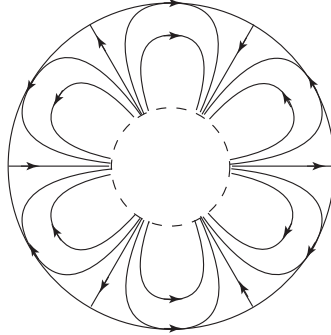


Figure 5.1. The phase portrait of (5.2) close to $\partial\mathbb{D}_r$ for r small and $\rho \ll r$.

with $s \in [0, 1]$, $\theta \in [0, 2\pi]$, $\alpha \in [0, 2\pi]$ and $\zeta \in [0, \rho)$. Then a rescaling $(z, t) \mapsto (\frac{z}{\zeta}, \zeta^k t)$ brings the system to the form

$$\frac{dZ}{dt} = U(Z) + O(\zeta), \quad (5.5)$$

where

$$U(Z) = Z \left(Z^k - k(1-s)^{k-1} e^{-i(k-1)\alpha} + (k-1)s^k e^{i(\theta-k\alpha)} \right),$$

i.e to a small perturbation of the system (2.5) studied above. However, the scaling transforms the domain \mathbb{D}_r into $\mathbb{D}_{r/\zeta}$ which tends to \mathbb{C} when $\zeta \rightarrow 0$.

PROPOSITION 5.1. — *Bifurcations of parabolic points occur along*

- (1) $\epsilon_0 = 0$: the bifurcation has codimension 1 if $\epsilon_1 \neq 0$, and codimension k otherwise;
- (2) $\Delta(\epsilon) = 0$, where $\Delta(\epsilon)$ is the discriminant of $Q_\epsilon(z)$. Note that

$$\Delta(\epsilon) = (-1)^{\lfloor \frac{k}{2} \rfloor} (k-1)^{k-1} k^k \left[\left(\frac{\epsilon_0}{k-1} \right)^{k-1} - \left(-\frac{\epsilon_1}{k} \right)^k + o(\|\epsilon\|^{k(k-1)}) \right]. \quad (5.6)$$

The bifurcation is of codimension 1 as soon as $\epsilon \neq 0$.

It is possible to generalize the definition of periodgon to this case.

DEFINITION 5.2 ([4]). — *Let $\dot{z} = \omega(z)$ be a holomorphic vector field in \mathbb{D}_r with all singular points simple.*

- (1) *The periodic domain in \mathbb{D}_r of a singular point z_j is the union of the periodic trajectories surrounding z_j for the rotated vector field $\dot{z} = e^{i \arg \nu_j} \omega(z)$, where $\nu_j = \frac{2\pi i}{\lambda_j}$. Its boundary is tangent to \mathbb{D}_r (see Figure 5.2 for some periodic domains in \mathbb{D}_r). The periodic domains of different points are disjoint.*

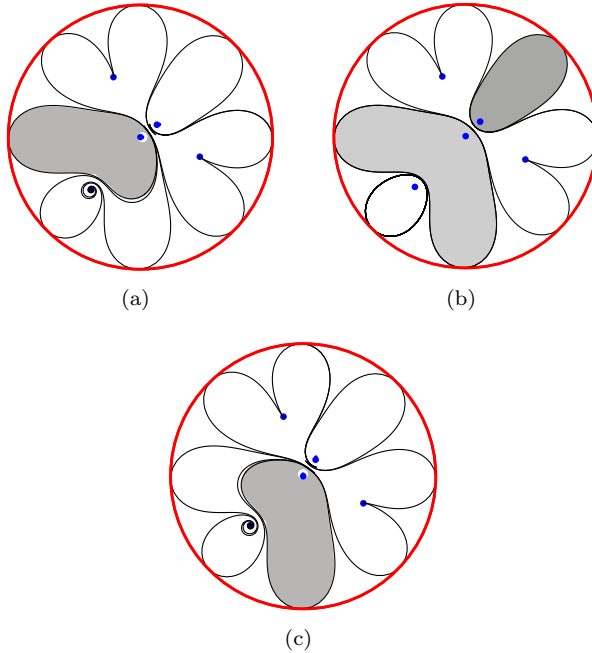


Figure 5.2. Some periodic domains in \mathbb{D}_r . The case (b) shows a bifurcation of the generalized periodgon between (a) and (c).

- (2) Let $t = \int \frac{dz}{\omega(z)}$. The generalized periodgon is the image in t -space of the complement in \mathbb{D}_r of the union of the periodic domains in \mathbb{D}_r (see Figure 5.3).

For generic values of the parameters there are, apart from the singular points, three kinds of generic trajectories inside \mathbb{D}_r :

- (1) Trajectories crossing $\partial\mathbb{D}_r$ with α - or ω -limit at a singular point (thick white trajectories in Figure 5.3(a));
- (2) Trajectories with α - and ω -limit at a singular point (thin white trajectories in Figure 5.3(a) and (c));
- (3) *Separating trajectories* entering and exiting \mathbb{D}_r (black trajectory in Figure 5.3(c)).

Non generic trajectories will have multiple tangency with the boundary $\partial\mathbb{D}_r$ (yellow trajectories in Figure 5.3(b) and (d)). Several of these trajectories replace the homoclinic loops in the bifurcation diagram.

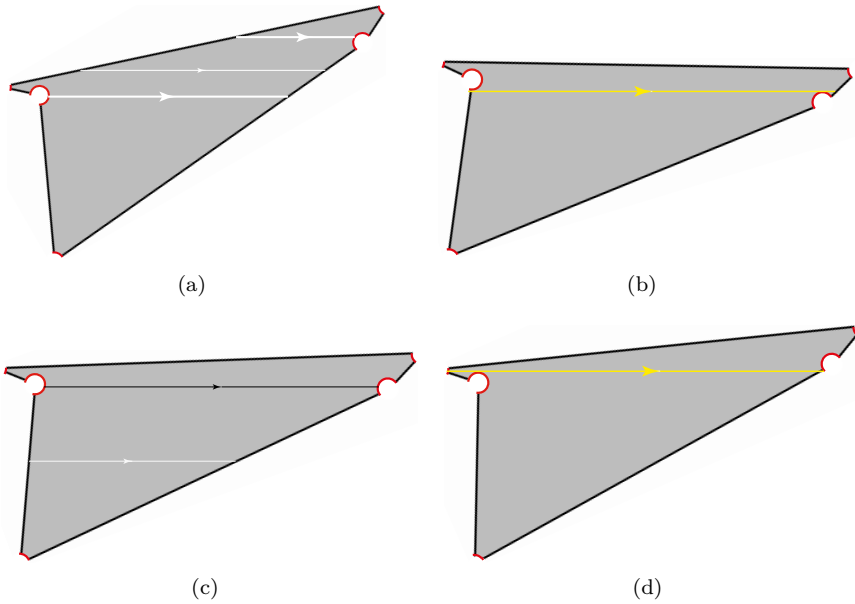


Figure 5.3. A generalized periodgon for $k = 4$ and different values of the rotational parameter α . The red parts of the boundary are images in t -space of arcs of $\partial\mathbb{D}_r$. In (c) a separating trajectory in black. The limit positions for separating trajectories are curves of double tangency with the boundary as in (b) and (d).

THEOREM 5.3. — *The bifurcation diagram of (5.2) consists of:*

- (1) *Bifurcations of parabolic points as described in Proposition 5.1.*
- (2) *Bifurcations of multiple tangencies of trajectories with the boundary $\partial\mathbb{D}_r$. Generically these are double tangencies. The corresponding bifurcation surfaces either limit regions in the parameter space in which there exist separating trajectories (see Figure 5.3) or regions where the generalized periodgon changes shape (see Figure 5.2(b)).*

Question. — It would be interesting to identify a unique normal form in which the parameters are uniquely defined (canonical). This was done in [4] when we drop the constraint that the origin is fixed in the unfolding. So far, we have not been able to find such a normal form in which the origin would be fixed. Such a normal form would lead to a classification theorem of germs of unfoldings (5.2) under conjugacy.

6. Appendix

THEOREM 6.1. — We consider a germ of m -parameter family f_ϵ unfolding a germ of diffeomorphism with a resonant fixed point of codimension k :

$$f_0(z) = \exp(2\pi ip/q)z + \frac{1}{q}z^{kq+1} + O(z^{kq+2}).$$

Then, there exists

- (1) a germ of change of coordinate conjugating f_ϵ to F_ϵ depending analytically on ϵ , for which each small periodic orbit of F_ϵ of order q is invariant under rotations of order q , i.e. all periodic points are roots of a polynomial $P_\epsilon(Z) = ZQ_\epsilon(Z^q)$;
- (2) and a polynomial $S_\epsilon(Z) = R_\epsilon(Z^q)$, where R_ϵ is a polynomial of degree at most k such that, for all periodic points Z_j of F_ϵ of order q , then $\log(F_\epsilon^{\circ q})'(Z_j) = \mu_j = P'_\epsilon(Z_j)S_\epsilon(Z_j)$, where μ_j is the eigenvalue at Z_j of the vector field $\dot{Z} = P_\epsilon(Z)S_\epsilon(Z_j)$.

The crucial step of the proof is the following theorem whose unpublished proof was communicated to us by Colin Christopher.

THEOREM 6.2 (Colin Christopher). — We consider a germ of family f_ϵ unfolding a germ of diffeomorphism with a resonant fixed point of codimension k :

$$f_0(z) = \exp(2\pi ip/q)z + \frac{1}{q}z^{kq+1} + O(z^{kq+2}).$$

Then, there exists a germ of change of coordinate $Z = h_\epsilon(z)$ conjugating f_ϵ to F_ϵ , for which each small periodic orbit of order q is invariant under rotations of order q , i.e.

$$F_\epsilon^{\circ q}(Z) - Z = P_\epsilon(Z)U(Z),$$

where $P_\epsilon(Z) = ZQ_\epsilon(Z^q)$ for some Weierstrass polynomial Q of degree k , and U is some unit.

Proof. — Let $\tau = \exp(2\pi ip/q)$, $f = f_\epsilon$, $g = f^{\circ q}$.

We need to symmetrize the fixed points, so the following change of coordinate is the obvious choice:

$$Z = h(z) = \frac{1}{q}(z + \tau^{-1}f(z) + \tau^{-2}f^{\circ 2}(z) + \dots + \tau^{-q+1}f^{\circ q}(z)).$$

The function h satisfies the functional equation

$$h(f(z)) = \tau h(z) + \frac{\tau}{q}(g(z) - z).$$

Let F (resp. G) be the map f (resp. g) in Z -coordinate. Then

$$F(Z) = h(f(h^{-1}(Z))) = \tau Z + \frac{\tau}{q}(g - \text{id}) \circ h^{-1}(Z) \quad (6.1)$$

And we can write $G(Z) - Z = P(Z)U_1(Z)$ for some Weierstrass polynomial P and some unit U_1 .

Now, $P(F(Z))$ has the same roots as $P(Z)$ (just the periodic points), so

$$P(F(Z)) = P(Z)U_2(Z), \quad (6.2)$$

for some unit U_2 . However, $(g - \text{id}) \circ h^{-1}(Z)$ also has the same roots as $P(Z)$ and hence (6.1) gives

$$F(Z) = \tau Z + V(Z)P(Z), \quad (6.3)$$

for some V (not necessarily a unit).

Hence, substituting from (6.3),

$$P(F(Z)) = P(\tau Z) + P(Z)N(Z), \quad (6.4)$$

for some function N .

Combining (6.2) and (6.4), we have

$$(U_2(Z) - N(Z))P(Z) = P(\tau Z),$$

so that $P(\tau Z)$ is an alternative Weierstrass polynomial to $P(Z)$. Since Weierstrass polynomials are unique, this yields as desired

$$P(Z) = P(\tau Z). \quad \square$$

End of proof of Theorem 6.1. — The rest of the proof is similar to the corresponding proof in [5]. For values of ϵ such that the roots of P_ϵ are distinct, there exists a polynomial S_ϵ of degree at most qk such that $\log(F_\epsilon^{\circ q})(Z_j) = P'_\epsilon(Z_j)S_\epsilon(Z_j)$. (S_ϵ is given by the Lagrange interpolation formula.) Moreover, S_ϵ is invariant under rotation of order q , and hence $S_\epsilon(Z) = R_\epsilon(Z^q)$ for some polynomial R_ϵ of degree at most k . S_ϵ can be extended on the discriminant locus of $P_\epsilon(Z)$. Indeed, it is bounded near the regular points of the discriminant locus (either a double periodic orbit or a periodic orbit merging with the fixed point) and Hartogs' theorem is used at the other points of the discriminant locus. \square

Acknowledgements

The author is grateful to Colin Christopher and Martin Klimeš for stimulating discussions.

Bibliography

- [1] A. CHÉRITAT & C. ROUSSEAU, “Generic 1-parameter perturbations of a vector field with a singular point of codimension k ”, <https://arxiv.org/abs/1701.03276>, 2017.
- [2] A. DOUADY, J.-F. ESTRADA & S. SENTENAC, “Champs de vecteurs polynomiaux sur \mathbb{C} ”, preprint, 2005.
- [3] A. G. KHOVANSKII, *Fewnomials*, Translations of Mathematical Monographs, vol. 88, American Mathematical Society, 1991, Translated from the Russian by Smilka Zdravkovska, viii+139 pages.
- [4] M. KLIMEŠ & C. ROUSSEAU, “Generic 2-parameter perturbations of parabolic singular points of vector fields in \mathbb{C} ”, *Conform. Geom. Dyn.* **22** (2018), p. 141-184.
- [5] C. ROUSSEAU, “Analytic moduli for unfoldings of germs of generic analytic diffeomorphisms with a codimension k parabolic point”, *Ergodic Theory Dyn. Syst.* **35** (2015), no. 1, p. 274-292.
- [6] ———, “The bifurcation diagram of cubic polynomial vector fields on $\mathbb{C}\mathbb{P}^1$ ”, *Can. Math. Bull.* **60** (2017), no. 2, p. 381-401.
- [7] C. ROUSSEAU & C. CHRISTOPHER, “Modulus of analytic classification for the generic unfolding of a codimension 1 resonant diffeomorphism or resonant saddle”, *Ann. Inst. Fourier* **57** (2007), no. 1, p. 301-360.